XI International Conference on Computational Plasticity. Fundamentals and Applications
COMPLAS XI
E. Oñate, D.R.J. Owen, D. Peric and B. Suárez (Eds)

IDENTIFICATION OF ORTHOTROPIC PLASTIC MATERIAL PARAMETERS FOR DEEP-DRAWING STEEL USING DIC AND FEMU

Stefan Schmaltz*, Kai Willner*

*Chair of Applied Mechanics, Department of Mechanical Engineering
Friedrich-Alexander University Erlangen-Nuremberg
Egerlandstr. 5, 91058 Erlangen, Germany
e-mail: stefan.schmaltz@ltm.uni-erlangen.de, willner@ltm.uni-erlangen.de
Web page: http://www.ltm.uni-erlangen.de

Key words: Computational Plasticity, Parameter Identification, Sheet steel, FEMU

Abstract. In this paper the deep-drawing sheet steel DC04, representative for sheet-bulk metal forming processes, is characterized through uni- and biaxial tensile and compression tests. The orthotropic plastic material parameters for the Hill 1948 yield surface are identified in two different ways. The first one utilizes uniaxial tensile experiments with specimen in three angles to the rolling direction of the sheet (0, 45 and 90 degree) and the plastic material parameters are calculated through the Lankford coefficients. Second a Finite Element Model Updating (FEMU) procedure is introduced. By taking the measured full-field displacement data and the forces of the biaxial tensile experiments better fitting parameters are identified at reasonable experimental costs.

1 INTRODUCTION

In engineering disciplines the complexity of produced parts and therewith of manufacturing processes increases steadily. In addition the product life cycle of many products gets shorter, which results in a need of reliable and fast numerical simulations. This coincides with the need of material parameters being optimized for the utilized material, load type and constitutive law.
The goal of our research is to present a procedure to get optimal material parameters at modest experimental costs. The chosen material, a deep-drawing sheet steel (DC04), which is representative for sheet-bulk metal forming processes, is characterized through uni- and biaxial tensile and compression tests. The plastic material parameters are identified in two different ways. At first the direct approach is taken, which uses the experimentally measured values of the different tests for the calculation of the yield surface. Then our Finite Element Model Updating (FEMU) procedure is introduced, applied and the results are discussed.

2 EXPERIMENTAL SET-UP AND DATA ACQUISITION

The used sheet metal is fabricated in a cold-rolling process and therefore shows orthotropic elastic and plastic material characteristics. To capture and verify this behavior, experiments based on different load types were performed, see fig. 1. For the uniaxial tensile test standardized specimen[1] were utilized. To prevent buckling the uniaxial compression test is performed on micro-specimen using hydraulic clamping with bearing extensions. In the biaxial tension and compression experiments a self-designed specimen is employed. Utilizing bearing plates, with friction reduction plates made out of Teflon®, in the biaxial compression tests, the initial compression yield point can be determined without buckling of the structure. The machines for the uniaxial testing are based on an

Figure 1: Specimen for the experimental testing

electro-mechanical principle. For the biaxial loading type a hydraulic machine is utilized where the cylinders of the vertical and horizontal axis can be controlled separately.

For the identification of the plastic material parameters with our FEMU procedure full-field displacement data and the experimentally determined forces of the experiments are essential. Therefore the deformation of the specimen during the experiments is captured with an optical full-field measurement system. On each specimen a stochastic spray pattern is applied which deforms with the specimen. In the course of the experiment a certain amount of pictures of the deforming specimen is taken and the full-field displacement data can be calculated through Digital Image Correlation (DIC).
There, a homogeneous mesh is layed onto the stochastic spray pattern in the initial state of the analysis. The elements are fitted to the deformed state by minimizing the deviation of the brightness distribution from previous to actual state. Having the elements in each state, the displacement field is identified.
Combined with each picture taken through the full-field measurement system the present force level is captured.

[1] Tensile Specimen DIN 50125 – H 12.5×50 of 2.0 mm sheet steel DC04

3 MATERIAL CHARACTERIZATION

The analyzed material shows orthotropic elastic and plastic characteristics without rate dependency. As sheet steel with a width of 2.0 mm is used, the plane stress element formulation is assumed to be valid. Having large deformation at small strains, the total strain $\boldsymbol{\epsilon}$ can be decomposed additively out of the elastic $\boldsymbol{\epsilon}^{\mathrm{el}}$ and the plastic part $\boldsymbol{\epsilon}^{\mathrm{pl}}$. In rate form this equation reads as

$$\dot{\boldsymbol{\epsilon}} = \dot{\boldsymbol{\epsilon}}^{\mathrm{el}} + \dot{\boldsymbol{\epsilon}}^{\mathrm{pl}}. \tag{1}$$

The elastic behavior is linear, utilizing Hooke's Law $\dot{\boldsymbol{\sigma}} = \boldsymbol{C}\dot{\boldsymbol{\epsilon}}^{\mathrm{el}} = \boldsymbol{C}(\dot{\boldsymbol{\epsilon}} - \dot{\boldsymbol{\epsilon}}^{\mathrm{pl}})$, with the stress tensor $\dot{\boldsymbol{\sigma}}$ in rate form and the compliance tensor $\boldsymbol{C}^{-1}$. The linearly independent, orthotropic elastic material parameters are identified by an iterative FEMU procedure to be $E_1 = 199,290\,\mathrm{MPa}$, $E_2 = 212,996\,\mathrm{MPa}$ and $\nu_{12} = 0.3356$. More detailed information can be found in [5]. The shear modulus G_{12} is defined as mean value.

$$\boldsymbol{C}^{-1} = \begin{bmatrix} \frac{1}{E_1} & -\frac{\nu_{12}}{E_1} & 0 \\ -\frac{\nu_{21}}{E_2} & \frac{1}{E_2} & 0 \\ 0 & 0 & \frac{1}{G_{12}} \end{bmatrix}, \quad \frac{\nu_{12}}{E_1} = \frac{\nu_{21}}{E_2}, \quad G_{12} = \frac{E_1 E_2}{E_1 + E_2 + 2\nu_{12}E_2} \tag{2}$$

For the solution of the inelastic part of the problem further equations have to be defined. To be able to describe the actual state internal variables Φ_i are applied. With their evolution equations

$$\dot{\Phi}_i = \dot{h}_i(\boldsymbol{\sigma}, \theta, \boldsymbol{\Phi}), \tag{3}$$

the yield function $F(\boldsymbol{\sigma}, \theta, \boldsymbol{\Phi}) = 0$ and the associative flow rule

$$\dot{\boldsymbol{\epsilon}}^{\mathrm{pl}} = \dot{\mu}\frac{\partial F}{\partial \boldsymbol{\sigma}}, \tag{4}$$

with the plastic multiplier $\dot{\mu}$, is defined. The plastic multiplier has to meet the following conditions

$$\dot{\mu}F = 0, \quad \dot{\mu} \geq 0, \quad F \leq 0. \tag{5}$$

As common practice for deep-drawing sheet steel, the orthotropic yield surface is modeled with the Hill 1948 ansatz [1]. It reads as:

$$F = a_1(\sigma_2 - \sigma_3)^2 + a_2(\sigma_3 - \sigma_1)^2 + a_3(\sigma_1 - \sigma_2)^2 + 3a_4\sigma_{31}^2 + 3a_5\sigma_{23}^2 + 3a_6\sigma_{12}^2 - 2\bar{\sigma}_{\mathrm{F}}^2. \tag{6}$$

The variables a_1 to a_6 describe the shape of the yield surface and $\bar{\sigma}_{\mathrm{F}}$ represents the current equivalent flow stress. For the plane stress configuration the Hill 1948 yield surface in the principal axes σ_1, σ_2 is described through an ellipse symmetric to the coordinate origin. The yield function reduces to

$$F = a_1\sigma_2^2 + a_2\sigma_1^2 + a_3(\sigma_1 - \sigma_2)^2 + 3a_6\sigma_{12}^2 - 2\bar{\sigma}_{\mathrm{F}}^2. \tag{7}$$

The remaining parameters a_1, a_2, a_3 and a_6 can be determined directly through evaluation of the Lankford coefficients $r^{(0°)}$, $r^{(45°)}$ and $r^{(90°)}$ from uniaxial tensile tests [1]. The Lankford coefficients, also called anisotropy parameters, are obtained by

$$r^{(d)} = \frac{\epsilon^{(d)}_{\text{width}}}{\epsilon^{(d)}_{\text{thickness}}}, \quad d = 0°, 45°, 90°. \tag{8}$$

The index d stands for the values of tensile tests with specimen from angles of 0, 45 and 90 degree to the rolling direction of the sheet metal.

The evolution of the yield surface, the hardening of the material, is modeled through a Hockett-Sherby law

$$\bar{\sigma}_{\text{F}}(\bar{\epsilon}_{\text{pl}}) = \bar{\sigma}_{\infty} - [\bar{\sigma}_{\infty} - \bar{\sigma}_0] \exp\left(A \cdot \bar{\epsilon}^{B}_{\text{pl}}\right). \tag{9}$$

In this equation $\bar{\sigma}_{\text{F}}$ represents the current equivalent flow stress, $\bar{\epsilon}_{\text{pl}}$ the current equivalent plastic strain, $\bar{\sigma}_{\infty}$ the equivalent stress to which the yield curve converges, $\bar{\sigma}_0$ the equivalent initial yield stress and A and B are further material parameters. The parameters vary for the different load types and are fitted individually with a curve fitting algorithm.

Utilizing the performed uniaxial tensile experiments the Hill 1948 initial yield surface for our sheet steel can be identified. It is plotted in fig. 2 and labeled as *Lankford*. In this

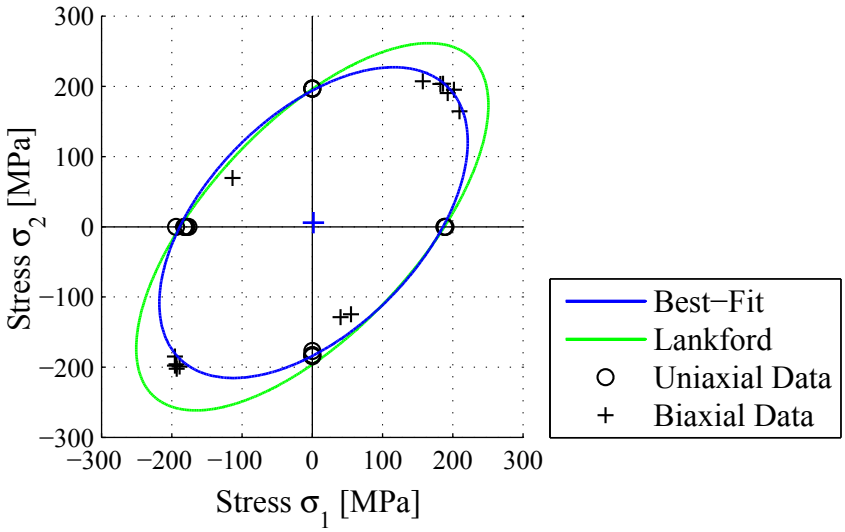

Figure 2: Experimentally determined Hill 1948 and *Best-Fit* yield surfaces

stress-stress diagram (fig. 2) also the initial yield stresses for the different experiments are plotted. To verify that the Hill 1948 yield surface is a sufficiently good model for our material a general ellipse equation is fitted to the experimental yield values. The

Best-Fit ellipse is obtained by a Least-Squares Fit using the Galerkin-Method to solve the overdetermined system of equations. The mid-point of the fitted ellipse lays almost in the coordinate origin as in the Hill 1948 model and the ellipse fits the data points very well.
Comparing the *Lankford* to the *Best-Fit* yield surface, a discrepancy for the biaxial yield stress can be found. To get a better fitting yield surface, without performing a large amount of experiments, our iterative FEMU procedure is utilized.

4 IDENTIFICATION PROCEDURE

For the identification procedure simulations of the performed experiments are set up. Here the biaxial tension test is chosen and modeled in the commercial Finite Element Method (FEM) software tool MSC.Marc. As having sheet metal, four-node, isoparametric, bilinear, plane-stress quadrilateral elements are utilized. The total amount of degrees of freedom is reduced by employing symmetric boundary conditions. The rolling direction is modeled through a rotation of the element coordinate system and the experimentally measured forces are applied as boundary condition, see fig. 3.

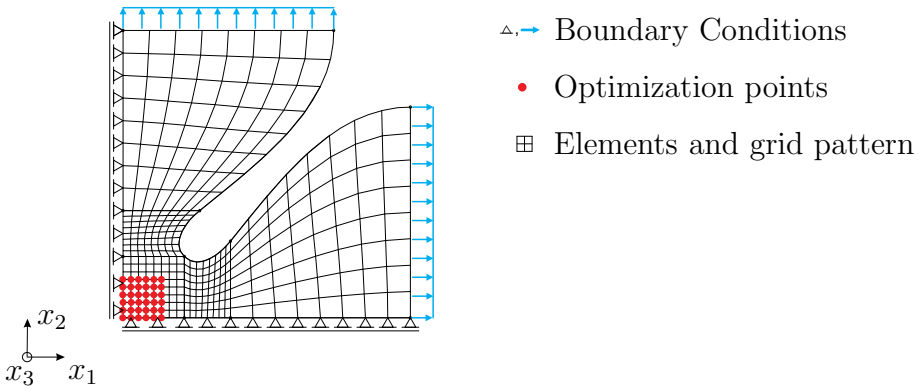

Figure 3: Modeled region of the biaxial tensile specimen

As we do have the measured full-field data sets and the simulations, the FEMU procedure for the parameter identification can be set up. Basic principles of the FEMU method and an overview over existing identification methods can be found in [2].
For our procedure the experimentally measured displacements u_1 and u_2 are required at a certain subset of nodes of the FE mesh. These optimization points are indicated in red in fig. 3. The values are calculated through a coordinate transformation and a data interpolation of the experimentally determined displacements.

The schedule of the FEMU procedure is depicted in fig. 4. It is controlled by an optimization routine which starts the FEMU procedure with a pre-defined set of initial material parameters. In our case the variational parameters are a_1, a_2, a_3 and a_6 of the plane stress Hill 1948 yield surface, see equation (7). With these parameters a FEM simu-

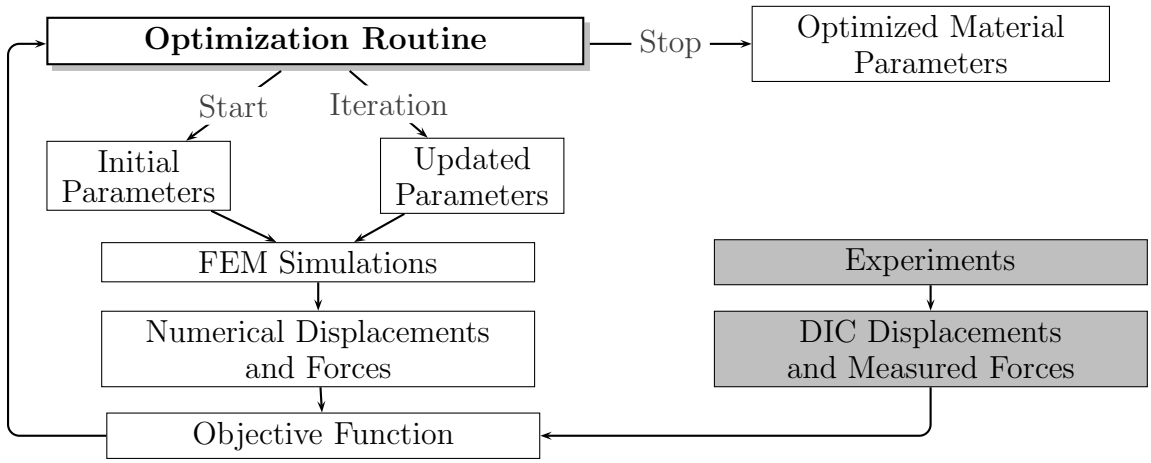

Figure 4: Schedule of the iterative FEMU procedure using experimental data

lation is run and the numerically and experimentally determined displacements and forces are processed by the objective function. Depending on the used optimization algorithm, a resulting vector or a scalar value is passed back to the optimization routine. If a certain stopping criterion is missed, the material parameters are updated and another iteration is initiated. Otherwise the optimized material parameters are identified which define the Hill 1948 yield surface.

The FEMU procedure is performed utilizing the biaxial tensile tests and their simulation.

5 PROCEDURE VERIFICATION

To verify the convergence of our identification procedure two optimization algorithms with different initial starting points are utilized [3]. The first algorithm is a gradient-free Nelder-Mead Simplex Method [4]. The utilized objective function $f(\boldsymbol{x}) = \Phi_{\mathrm{U}}(\boldsymbol{x}) + \Phi_{\mathrm{K}}(\boldsymbol{x})$ is a sum of the weighted least-squares sums of the experimentally and numerically determined displacements (10) and the forces (11).

$$\Phi_{\mathrm{U}}(\boldsymbol{x}) = \frac{1}{2NM} \sum_{i=1}^{M} \sum_{j=1}^{N} \sum_{k=1}^{2} w_{\mathrm{U},k} \left[(u_k^{(\mathrm{exp})})_{ij} - (u_k^{(\mathrm{num})}(\boldsymbol{x}))_{ij} \right]^2 \tag{10}$$

$$\Phi_{\mathrm{K}}(\boldsymbol{x}) = w_{\mathrm{K}} \frac{1}{M} \sum_{i=1}^{M} \left[(K^{(\mathrm{exp})})_i - (K^{(\mathrm{num})}(\boldsymbol{x}))_i \right]^2 \tag{11}$$

In the equations (10) and (11) $u_k^{(\ldots)}$ are the displacements, K are the forces and $w_{\mathrm{U},1}$, $w_{\mathrm{U},2}$ and w_{K} are the weighing factors. The indices stand for the steps in the numerical simulation (i), the number of optimization points (j) and the space directions (k).
The second optimization algorithm is the gradient-based Levenberg-Marquardt Trust Region Method [4]. An approximation of the objective function is minimized in a certain

Trust Region r, see equation (12).

$$\min_{\boldsymbol{s}} \frac{1}{2}\|\boldsymbol{J}(\boldsymbol{x})\boldsymbol{s} + \boldsymbol{v}(\boldsymbol{x})\|_2^2, \text{ subject to } \|\boldsymbol{s}\| \leq r \tag{12}$$

$$v_i(\boldsymbol{x}) = \begin{cases} w_{\mathrm{U},k}\left[(u_k^{(\mathrm{exp})})_i - (u_k^{(\mathrm{num})}(\boldsymbol{x}))_i\right], & \text{for } 1 \leq i < l. \\ w_{\mathrm{K}}\left[(K^{(\mathrm{exp})})_i - (K^{(\mathrm{num})}(\boldsymbol{x}))_i\right], & \text{for } l \leq i < m. \end{cases} \tag{13}$$

The parameter $v_i(\boldsymbol{x})$ is a column vector of the weighted least-squares sums of the forces and the displacements and $\boldsymbol{J}(\boldsymbol{x}) = \left[\frac{\partial v_j}{\partial x_i}\right]$ is its Jacobian. The value l is the number of steps times the number of optimization points and $(m-l)$ represents the number of steps. As no gradient is accessible in the used commercial FE code it is calculated through an evaluation of Finite Differences.

In order to show that the above described identification setup is reasonable and to test the FEMU procedure a numerical experiment is performed. An orthotropic Hill 1948 yield surface which is conform to the *Best-Fit* ellipse is defined. Boundary conditions equal to the measured ones of the biaxial tensile tests are applied and the resulting displacements and forces are recorded. Then a FEMU procedure is initiated. The numerically determined forces and displacements are taken as input-data and the parameters a_1, a_2, a_3 and a_6 are re-identified. Table 1 shows the pre-defined material parameters and the identified ones with the FEMU procedures with their standard deviations. Two runs were performed. In the first FEMU procedure the gradient-based Levenberg-Marquardt optimization algorithm is utilized. In order to verify the convergence of our procedure, three different initial starting parameter sets are employed, see fig. 5. The three runs converge to the same results with a small standard deviation (table 1). In the second FEMU cycle

Table 1: Identified material parameters of the numerical example from gradient-free and gradient-based methods with standard deviation

	a_1	a_2	a_3	a_6
Pre-defined Parameters	9.38e-01	9.49e-01	1.02e+00	1.10e+00
Ident. Param. gradient-based	9.40e-01	9.51e-01	1.02e+00	1.09e+00
Standard Deviation	1.82e-03	2.12e-03	2.77e-03	2.05e-02
Ident. Param. gradient-free	9.32e-01	9.43e-01	1.02e+00	1.09e+00
Standard Deviation	5.07e-03	5.42e-03	4.22e-03	3.29e-02

the gradient-free Nelder-Mead Simplex optimization algorithm is employed. This algorithm is started with three different initial material parameter sets. It converges to the values shown in table 1. However, the number of function evaluations needed to converge is higher than the one of the gradient-based algorithm and convergence is reached only if the initial parameters are within a small region around the optimal values.

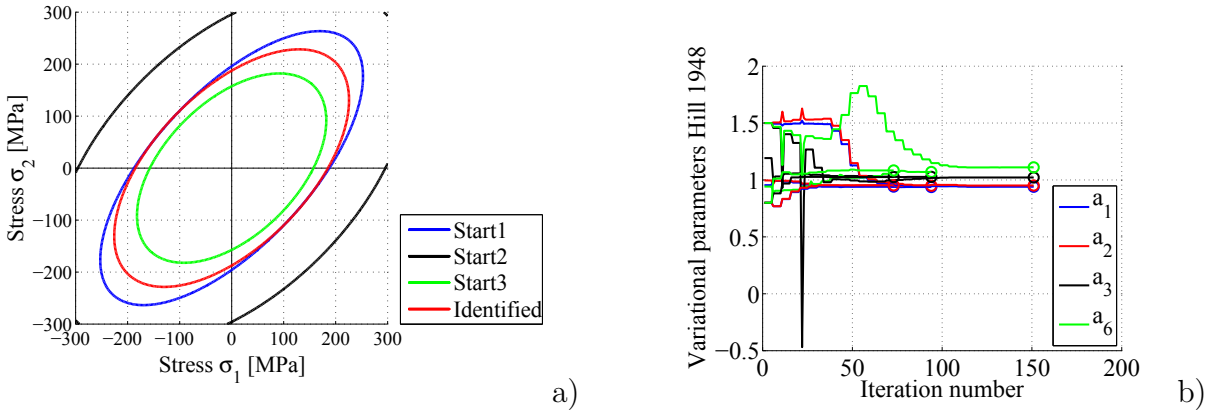

Figure 5: Numerical biaxial tension experiment, gradient-based method: **a)** Initial and identified yield surfaces. **b)** Variational parameters over iteration number.

6 IDENTIFIED PARAMETERS

Having verified that our FEMU procedure is capable of identifying the proper orthotropic plastic material parameters the experimentally determined displacements and forces of three biaxial tension tests are employed as input data. As in the numerical example the FEMU procedure is run with the two optimization algorithms starting from different initial material parameter sets. Fig. 6a) depicts that four different starting sets are utilized. Comparing fig. 6b) to fig. 5b) it is obvious that the convergence with the experimental data set is faster. This effect is caused by the inhomogeneities in the measured

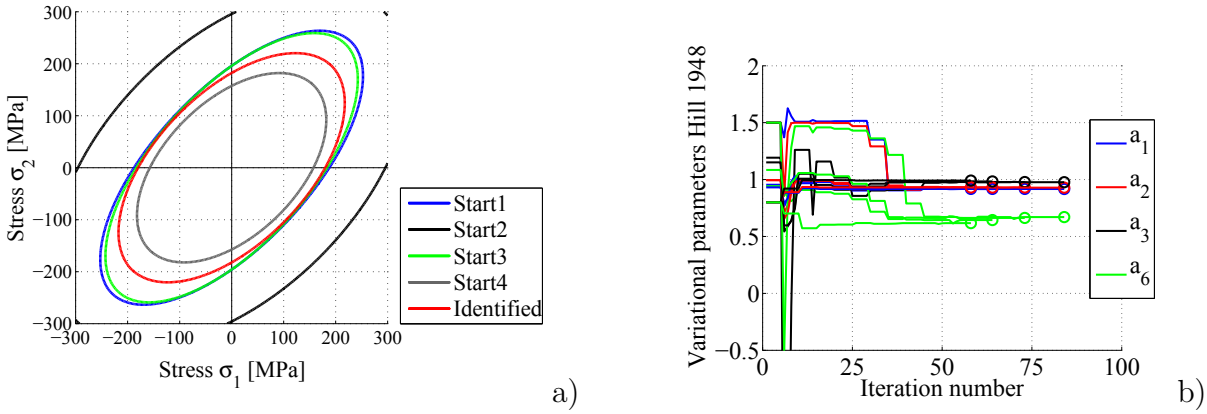

Figure 6: Biaxial tension experiment, gradient-based method: **a)** Initial and identified yield surfaces. **b)** Variational parameters over iteration number.

data. As being not perfectly biaxially loaded over all time steps, like in the numerical

example, and using three different experimental data sets in one FEMU procedure the iteration number decreases.
The identified material parameters for the Hill 1948 yield surface are written down in table 2. The standard deviations of the gradient-free optimization cycles are smaller than the gradient-based ones. However, convergence with the gradient-free method is reached only if good starting parameter sets are chosen.

Table 2: Identified material parameters of the experimental data sets from gradient-free and gradient-based methods with standard deviation

	a_1	a_2	a_3	a_6
Ident. Param. gradient-based	9.18E-01	9.30E-01	9.82E-01	6.49E-01
Standard Deviation	4.82E-04	6.28E-04	6.36E-03	2.37E-02
Ident. Param. gradient-free	9.18e-01	9.30e-01	9.78e-01	6.64e-01
Standard Deviation	1.61e-03	6.82e-04	1.57e-03	6.11e-03

Fig. 7 depicts the via FEMU identified Hill 1948 yield surface together with the *Lankford* and *Best-Fit* surfaces. Especially the biaxial yield stress is represented more accurately as through the *Lankford* yield surface. Therewith only biaxial tensile tests are

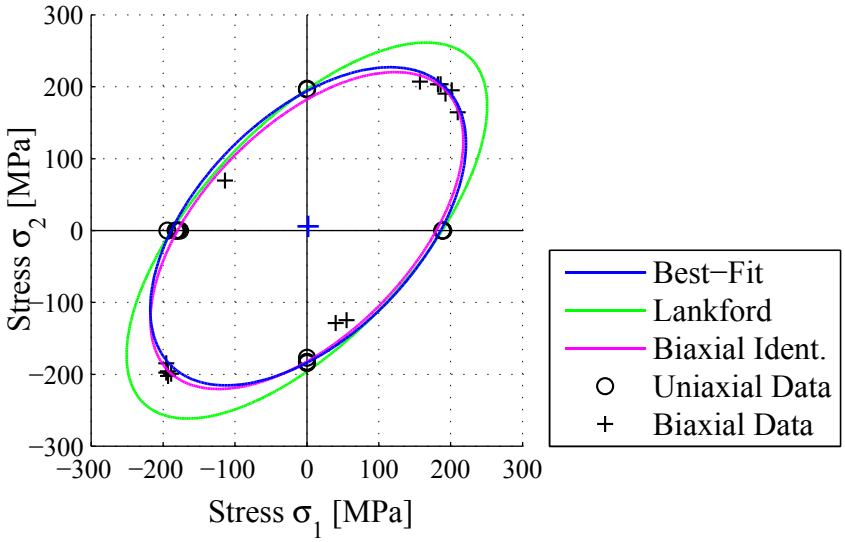

Figure 7: Identified Hill 1948 yield surface

needed to be able to identify the initial yield surface almost as precisely as performing various different tensile and compression experiments and fitting a general ellipse to this data set.

7 CONCLUSION AND OUTLOOK

The paper characterizes the orthotropic plastic behavior of the sheet steel DC04 through uni- and biaxial tension and compression tests. The plastic material parameters for the Hill 1948 yield criterion are identified directly and by an iterative FEMU procedure employing full-field displacement data and forces from experiments. Utilizing this FEMU procedure the amount of experiments needed for the material characterization is minimized, while the accurateness of the identified material parameters is maximized.
In order to accelerate the convergence and to increase the precision more complex specimen resulting in inhomogeneous loading are to be generated. Furthermore a combined anisotropic and kinematic hardening function has to be implemented to be able to represent the hardening behavior of the sheet metal more accurately.

Acknowledgements. This work is supported by the German Research Foundation (DFG) under the Transregional Collaborative Research Centre SFB/TR73.

REFERENCES

[1] Lecompte, D. et al., Identification of yield locus parameters of metals using inverse modeling and full field information, *Proc. of the 7th USNCTAM*, (2006).

[2] Avril, S. et al., Overview of Identification Methods of Mechanical Parameters Based on Full-field Measurements, *Exp. Mech.*, (2008) **48**: 381–402

[3] Chaparro, B.M. et al., Material parameters identification: Gradient-based, genetic and hybrid optimization algorithms, *Comp. Mater. Sci.*, (2008) **44**: 339–346.

[4] Nocedal, J., Wright, S. J., Numerical Optimization (Second Edition), *Springer Science+Business Media, New York*, (2006).

[5] Schmaltz, S., Willner, K., Optimization of elastic material parameters of sheet metal with FEMU and DIC, Submitted to: *PAMM*, (2011)